

## Supplementary Information

### Interface Diagnostics Platform for Thin-Film Solid-State Batteries

Victoria C. Ferrari, Sang Bok Lee, Gary W. Rubloff, David M. Stewart

#### Part 1: fundamental equations to build analytical solutions for the electric circuit models

The impedance of a Constant-Phase Element (CPE) is described by the following equation:

$$Z_{CPE}(\omega) = \frac{1}{(j\omega)^a Q} = \frac{\cos\left(\frac{\pi}{2}a\right)}{\omega^a Q} - j \frac{\sin\left(\frac{\pi}{2}a\right)}{\omega^a Q} \quad (\text{S1})$$

Where  $\omega$  is the angular frequency (rad/s),  $Q$  has units of  $\text{F/s}^{1-a}$ , and  $a$  is unitless. From equation (S1), the impedance of a CPE has both real and imaginary parts that are frequency-dependent, such that:

$$\text{Re}\{Z_{CPE}\} = Z' = \frac{\cos\left(\frac{\pi}{2}a\right)}{\omega^a Q} \quad (\text{S2})$$

$$\text{Im}\{Z_{CPE}\} = Z'' = -\frac{\sin\left(\frac{\pi}{2}a\right)}{\omega^a Q} \quad (\text{S3})$$

And the magnitude of the impedance can be calculated as well:

$$|Z_{CPE}| = \sqrt{Z'^2 + Z''^2} = \frac{1}{\omega^a Q} \quad (\text{S4})$$

In practice,  $a$  ranges from 0.5 (ideal diffusion mechanism<sup>1</sup>) to 1 (ideal capacitor behavior). The use of CPEs accommodate the possible inhomogeneities of materials' fabrication, porosity, and roughness of solid-solid interfaces<sup>2</sup>. While  $Q$  has similarities with a capacitance ( $C$ ), they are not equal<sup>3</sup>. Nevertheless, it is possible to calculate a corresponding capacitance of a CPE from the impedance equation for a capacitor:

$$C = \frac{1}{j\omega Z} = -j \frac{1}{\omega Z} \quad (S5)$$

And therefore:

$$C_{CPE}(\omega) = -j \frac{1}{\omega Z_{CPE}} = C'(\omega) + jC''(\omega) \quad (S6)$$

Hence, when modeling materials that require the use of a CPE, its equivalent capacitance is a complex number<sup>4</sup>. Equation ( S6 ) can be further derived in terms of  $Z_{CPE}$  to calculate the real and imaginary parts of the capacitance using equations ( S2 ), ( S3 ) and ( S4 ):

$$C'(\omega) = -\frac{1}{\omega} \frac{Z''}{|Z|^2} = \frac{Q}{\omega^{1-a}} \sin\left(\frac{\pi}{2} a\right) \quad (S7)$$

$$C''(\omega) = -\frac{1}{\omega} \frac{Z'}{|Z|^2} = -\frac{Q}{\omega^{1-a}} \cos\left(\frac{\pi}{2} a\right) \quad (S8)$$

Therefore,  $C$  is directly proportional to  $Q$ , and equations ( S7 ) and ( S8 ) also show the relation between the capacitance and the frequency.

The bulk capacitance of a layer is directly related to the geometry of the device, and it is delimited by the thickness of the material ( $d$ ), active area ( $A$ ), vacuum permittivity ( $\epsilon_0$ ) and its relative permittivity ( $\epsilon_r$ ) for the case of a parallel-plate capacitor, according to equation ( S9 ):

$$C_{Bulk}(\omega) = \frac{\epsilon_r \epsilon_0 A}{d} \Rightarrow \epsilon_r = \left(\frac{d}{\epsilon_0 A}\right) C_{Bulk}(\omega) = \epsilon_r'(\omega) + j\epsilon_r''(\omega) \quad (S9)$$

Where  $\epsilon_r$  has a frequency dependence due to the nature of the complex capacitance, which can be computed using equations ( S7 ), ( S8 ) and ( S9 ):

$$\epsilon_r'(\omega) = \left(\frac{d}{\epsilon_0 A}\right) C'_{Bulk}(\omega) = \left(\frac{d}{\epsilon_0 A}\right) \frac{Q}{\omega^{1-a}} \sin\left(\frac{\pi}{2} a\right) \quad (S10)$$

$$\varepsilon_r''(\omega) = \left(\frac{d}{\varepsilon_0 A}\right) C_{Bulk}''(\omega) = -\left(\frac{d}{\varepsilon_0 A}\right) \frac{Q}{\omega^{1-a}} \cos\left(\frac{\pi}{2} a\right) \quad (S11)$$

From the real and imaginary components of the relative permittivity complex number, the real part, indicated by equation ( S10 ), corresponds to the dielectric function, while the ratio between the imaginary part and the real part is called the dielectric loss<sup>5,6</sup>. The dielectric function decreases at high frequencies because of the reduced space-charge polarization effect. The dielectric loss is directly related to the electromagnetic energy loss due to the nature of the material in the presence of an applied electrical field<sup>7</sup>.

At interfaces (and interphases), charges can be accumulated or depleted according to the applied bias. CPEs are implemented to model this charge dynamics at different heterojunctions in a thin-film device, and the width of these created space-charge layers ( $d_{SCL}$ ) can be derived from equation ( S10 ):

$$d_{SCL} = \frac{\varepsilon_r'(\omega) \varepsilon_0 A}{C'_{interface}(\omega)} \quad (S12)$$

Like the relative permittivity and the capacitance,  $d_{SCL}$  is mathematically frequency-dependent. In practice, accumulation of charges and depletion of them will be studied at minimum frequencies for evaluation of the effect of SCL during charge-transfer reactions. Here, the minimum frequency used during the electrochemical measurements was 250 mHz, which was the selected frequency for estimation of  $d_{SCL}$ .

## Part 2: Error propagation of derived parameters

Some properties of materials were calculated using geometrical values (active surface area and film thickness) and also parameters extracted from the electric circuit modeling. Hence, those properties have associated uncertainties that were calculated based on error propagation.

### a) Uncertainty of a CPE capacitance ( $\sigma_{C'}$ )

From equation ( S7 ), the real part of the capacitance of a CPE has an uncertainty that depends on the parameters  $a$  and  $Q$ :

$$\sigma_{C'} = \sqrt{\sigma_a^2 \left( \frac{\partial C'}{\partial a} \right)^2 + \sigma_Q^2 \left( \frac{\partial C'}{\partial Q} \right)^2}$$

( S13 )

Where  $\sigma_a$  and  $\sigma_Q$  are the fitting errors of  $a$  and  $Q$  parameters. Equation ( S13 ) can be simplified using the value of the imaginary part of the capacitance from equation (8):

$$\sigma_{C'} = \sqrt{\sigma_a^2 \left[ \ln(\omega) C' - \frac{\pi}{2} C'' \right]^2 + \sigma_Q^2 \left( \frac{C'}{Q} \right)^2}$$

( S14 )

b) Uncertainty of relative permittivity ( $\sigma_{\epsilon'_r}$ )

The relative permittivity ( $\epsilon_r$ ) of a material depends on its bulk capacitance,  $C_{Bulk}$ , surface area  $A$ , and thickness  $d$ , according to equation ( S10 ). For this error estimation, the associated area error was neglected since  $A$  could be determined by the design of devices and it was easily measured. The uncertainty of  $C_{Bulk}$  was calculated using equation ( S14 ), and the thickness error was estimated from cross-sectional measurements taken by SEM. Hence, only  $C_{Bulk}$  and  $d$  will contribute to the uncertainty of the  $\epsilon_r$ :

$$\sigma_{\epsilon'_r} = \sqrt{\sigma_{C'_{Bulk}}^2 \left( \frac{\partial \epsilon'_r}{\partial C'_{Bulk}} \right)^2 + \sigma_d^2 \left( \frac{\partial \epsilon'_r}{\partial d} \right)^2}$$

( S15 )

Which can be further derived into the following equation:

$$\sigma_{\epsilon'_r} = \epsilon'_r \sqrt{\left( \frac{\sigma_{C'_{Bulk}}}{C'_{Bulk}} \right)^2 + \left( \frac{\sigma_d}{d} \right)^2}$$

( S16 )

c) Uncertainty of the width of space-charge layer ( $\sigma_{d_{SCL}}$ )

From equation ( S12 ),  $d_{SCL}$  depends on the relative permittivity of the material, its surface area and interfacial capacitance. Using equations ( S14 ) and ( S16 ), the associated error of  $d_{SCL}$  can be calculated as:

$$\sigma_{d_{SCL}} = \sqrt{\sigma_{C'_{Interface}}^2 \left( \frac{\partial d_{SCL}}{\partial C'_{Interface}} \right)^2 + \sigma_{\epsilon'_r}^2 \left( \frac{\partial d_{SCL}}{\partial \epsilon'_r} \right)^2} \quad (S17)$$

Which is simply calculated as:

$$\sigma_{d_{SCL}} = d_{SCL} \sqrt{\left( \frac{\sigma_{C'_{Interface}}}{C'_{Interface}} \right)^2 + \left( \frac{\sigma_{\epsilon'_r}}{\epsilon'_r} \right)^2} \quad (S18)$$

d) Uncertainty of ionic and electronic conductivities of bulk materials and interfaces ( $\sigma_{\sigma_e}, \sigma_{\sigma_i}$ )

From equation (1) of the main text, the associated error of conductivity calculations will depend on the resistance (R) and the thickness (d) of the layer. For bulk materials, d was measured by cross-sectional SEM images:

$$\sigma_{\sigma_{Bulk}} = \sigma_{Bulk} \sqrt{\left( \frac{\sigma_{d_{Bulk}}}{d_{Bulk}} \right)^2 + \left( \frac{\sigma_{R_{Bulk}}}{R_{Bulk}} \right)^2} \quad (S19)$$

For interfaces/interphases, d corresponds to the space-charge layer that was calculated using equations ( S12 ) and ( S18 ):

$$\sigma_{\sigma_{interface}} = \sigma_{interface} \sqrt{\left( \frac{\sigma_{d_{SCL}}}{d_{SCL}} \right)^2 + \left( \frac{\sigma_{R_{interface}}}{R_{interface}} \right)^2} \quad (S20)$$

### Part 3: Specific considerations of the electric circuit model for LiPON-only device

Charge dynamics can be predicted in this metal-electrolyte-metal system according to the diffusivity of ionic species (like  $Li^+$ ) in two different regimes: bulk domain and interfacial domain.

When the frequencies of the input sinusoidal voltage from PEIS are large enough, less time is given for  $\text{Li}^+$  to diffuse inside the electrolyte, and they tend to get localized, which contributes to bulk polarization. In this case (bulk domain), accumulation of ion charges at the Electrolyte-Metal Interfaces (EMIs) is very small or nonexistent. When the frequencies are small (interfacial domain),  $\text{Li}^+$  are diffusing according to the applied electric field, with no significant bulk polarization while the charge polarization happens mainly at the EMIs.

CPEs can be used to model both the bulk polarization and the local accumulation of charges at the interfaces with metal layers. Denoting  $\text{CPE}_{\text{electrolyte}}$  and  $\text{CPE}_{\text{interface}}$  as the electrical parameters that will model the bulk and interfacial charge polarization, these CPEs will have different behaviors under different frequency ranges, which can be represented by their association in parallel.  $R_{\text{electrolyte}}$ , i.e., the electrolyte resistance of  $\text{Li}^+$ , should have a series association with  $\text{CPE}_{\text{interface}}$  because these two processes (diffusion and charge accumulation/depletion at EMIs) occur in a sequential progression at lower frequencies. Figure S1 illustrates the complete electric circuit modelling for the Al/LiPON/Cu device derived from the physical considerations and aforementioned approximations.

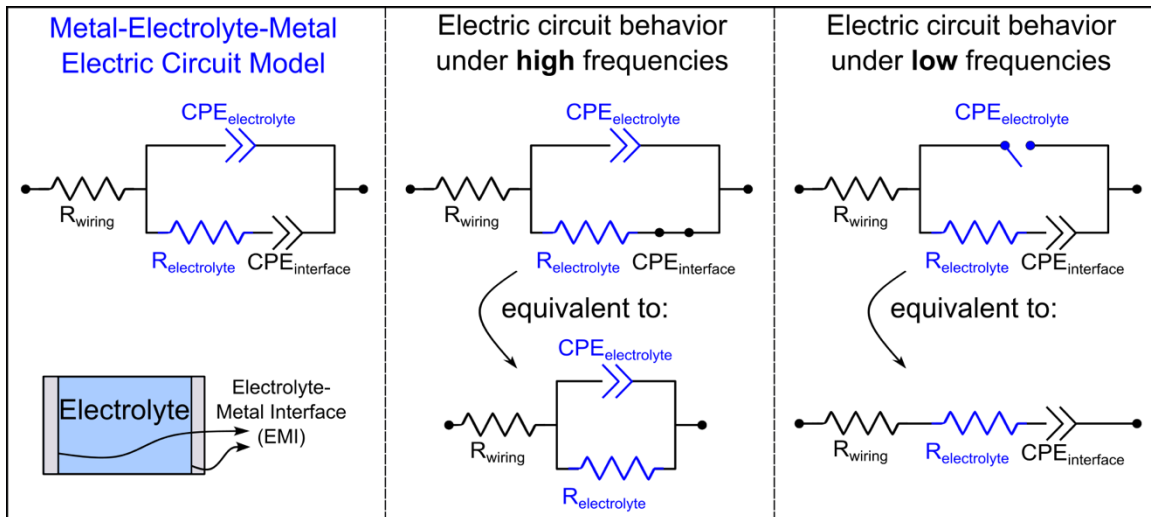


**Figure S1.** Visual description of the Al/LiPON/Cu electric circuit model and its equivalency under different frequencies.

Therefore, at lower frequencies, the series association of resistances and  $\text{CPE}_{\text{interface}}$  results in a “diffusion tail” in a Nyquist plot, which should be a straight line parallel to the y-axis if such interface could be modeled as an ideal capacitor. For CPEs with a smaller than 1, that

diffusion tail will have an angle with respect to the x-axis that arises from the frequency-dependent real impedance showed in equation S2. At high frequencies, the parallel  $R_{\text{electrolyte}}/CPE_{\text{electrolyte}}$  association will result in a depressed semicircle shape in a Nyquist plot (which eccentricity depends on factor  $a$ ). That arc, at extremely elevated frequencies, would intercept zero at the x-axis, but the presence of a finite resistance due to the wiring ( $R_{\text{wiring}}$ ) shifts the arc to this resistance value.

### Part 3: Specific considerations of the electric circuit model for LVO-only device

The conduction of electrons in the anode and in the cathode should be comparable to the conduction of  $\text{Li}^+$  in them. Therefore, the electric circuit model of a metal-electrode-metal device should include an extra resistor ( $R_{\text{electronic}}$ ) in the electric circuit shown in Figure S2 to properly model the electric pathway for electronic conduction. Since electrons and  $\text{Li}^+$  will be flowing in opposite directions,  $R_{\text{electronic}}$  is connected in parallel to the resistor that models the ionic conduction inside an electrode ( $R_{\text{ionic}}$ ).

Although  $\text{Li}^+$  will still be blocked at interfaces due to the ion-blocking nature of the chosen metals to serve as current collectors, electrons will be allowed to be transferred from the electrode to the metal layer and vice-versa, according to the direction of the generated electric field. Hence, it is expected that electrons will not be able to reach the electrode-metal interface at high frequencies, and less accumulation of charges might happen at this interface under lower frequencies since there is an electronic charge transfer. The electric circuit model from Figure S2 considers all of these physical processes with respect to conduction of ions and electrons inside an electrode, and the electronic charge transfer at interfaces.

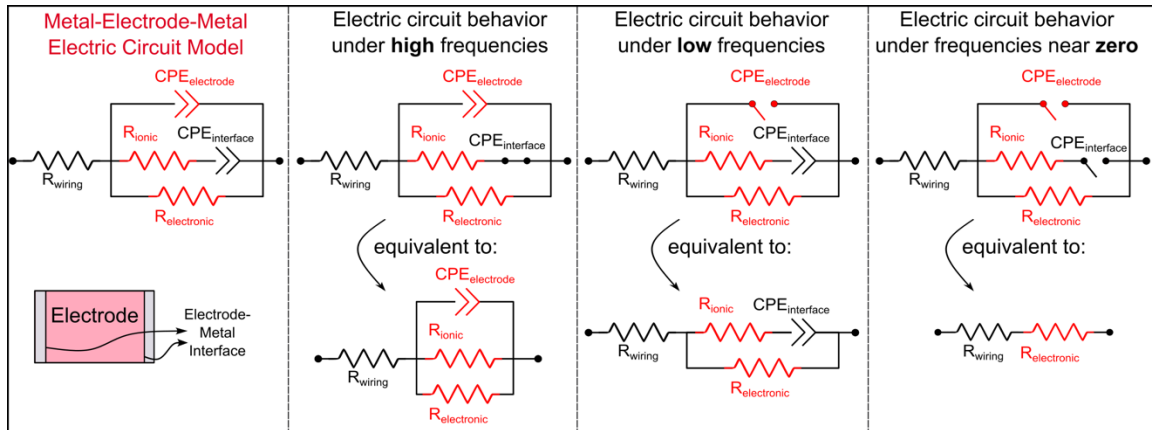


**Figure S2:** Al/LiPON/Cu electric circuit model and its equivalency under different frequencies.

## References

1. Randles, J. E. B. Kinetics of rapid electrode reactions. *Discuss. Faraday Soc.* **1**, 11 (1947).
2. Nara, H., Yokoshima, T. & Osaka, T. Technology of electrochemical impedance spectroscopy for an energy-sustainable society. *Curr. Opin. Electrochem.* **20**, 66–77 (2020).
3. Orazem, M. E. *et al.* Dielectric Properties of Materials Showing Constant-Phase-Element (CPE) Impedance Response. *J. Electrochem. Soc.* **160**, C215–C225 (2013).
4. Ahuja, K. *et al.* Ultra-thin on-chip ALD LiPON capacitors for high frequency application. *J. Power Sources* **575**, 233056 (2023).
5. Kadri, E. *et al.* Ac conductivity and dielectric behavior of a – Si : H / c – Si  $1 - y$  Ge  $y$  / p – Si thin films synthesized by molecular beam epitaxial method. *J. Alloys Compd.* **705**, 708–713 (2017).
6. Sallaz, V., Oukassi, S., Voiron, F., Salot, R. & Berardan, D. Assessing the potential of LiPON-based electrical double layer microsupercapacitors for on-chip power storage. *J. Power Sources* **451**, 227786 (2020).
7. Gaabour, L. H. Study of the structural, AC electrical conductivity, electric modulus, and dielectric properties of novel PVDF/LiCoO<sub>2</sub> nanocomposites for Li-ion batteries. *AIP Adv.* **11**, 095114 (2021).